Received: 27 March 2023 | Revised: 15 September 2023 | Accepted: 3 October 2023

DOI: 10.1111/gcb.17018

Global Change Biology WILEY

RESEARCH ARTICLE

Shift in algal blooms from micro- to macroalgae around China with increasing eutrophication and climate change

Yuan Feng[1] | Yonglong Xiong[1] | Jason M. Hall-Spencer[2,3] | Kailin Liu[4] | John Beardall[1,5,6] | Kunshan Gao[1] | Jingke Ge[1] | Juntian Xu[7] | Guang Gao[1]

[1]State Key Laboratory of Marine Environmental Science & College of Ocean and Earth Sciences, Xiamen University, Xiamen, China

[2]Marine Institute, University of Plymouth, Plymouth, UK

[3]Shimoda Marine Research Center, Tsukuba University, Tsukuba, Japan

[4]College of the Environment & Ecology, Xiamen University, Xiamen, China

[5]School of Biological Sciences, Monash University, Clayton, Victoria, Australia

[6]Faculty of Applied Sciences, UCSI University, Kuala Lumpur, Malaysia

[7]Jiangsu Key Laboratory for Marine Bioresources and Environment, Jiangsu Ocean University, Lianyungang, China

Correspondence
Guang Gao, State Key Laboratory of Marine Environmental Science & College of Ocean and Earth Sciences, Xiamen University, Xiamen 361005, China.
Email: guang.gao@xmu.edu.cn

Funding information
National Key Research and Development Program of China, Grant/Award Number: 2022YFC3105304; National Natural Science Foundation of China, Grant/Award Number: 42076154; Natural Resources Development (Innovation Project of Marine Science and Technology) of Jiangsu Province, Grant/Award Number: JSZRHYKJ202206; Royal Society China-UK International Exchanges, Grant/Award Number: IEC\NSFC\181187; Japan Society for the Promotion of Science ICONA Program, Grant/Award Number: JPJSCCA20210006

Abstract

Blooms of microalgal red tides and macroalgae (e.g., green and golden tides caused by *Ulva* and *Sargassum*) have caused widespread problems around China in recent years, but there is uncertainty around what triggers these blooms and how they interact. Here, we use 30 years of monitoring data to help answer these questions, focusing on the four main species of microalgae *Prorocentrum donghaiense*, *Karenia mikimotoi*, *Noctiluca scintillans*, and *Skeletonema costatum*) associated with red tides in the region. The frequency of red tides increased from 1991 to 2003 and then decreased until 2020, with *S. costatum* red tides exhibiting the highest rate of decrease. Green tides started to occur around China in 1999 and the frequency of green tides has since been on the increase. Golden tides were first reported to occur around China in 2012. The frequency of macroalgal blooms has a negative linear relationship with the frequency and coverage of red tides around China, and a positive correlation with total nitrogen and phosphorus loads as well as with atmospheric CO_2 and sea surface temperature (SST). Increased outbreaks of macroalgal blooms are very likely due to worsening levels of eutrophication, combined with rising CO_2 and SST, which contribute to the reduced frequency of red tides. The increasing grazing rate of microzooplankton also results in the decline in areas affected by red tides. This study shows a clear shift of algal blooms from microalgae to macroalgae around China over the past 30 years driven by the combination of eutrophication, climate change, and grazing stress, indicating a fundamental change in coastal systems in the region.

KEYWORDS
CO_2, eutrophication, golden tides, green tides, red tides, warming

1 | INTRODUCTION

Red tides are a type of harmful algal bloom that redden seawater due to the rapid multiplication of phytoplankton including dinoflagellates, diatoms, and cyanobacteria (Anderson, 2009). Toxins produced by red tides, even at relatively low cell densities, can cause illness and mortality in fish, seabirds, and marine mammals (Hallegraeff, 2010). People can also be poisoned if they eat seafood contaminated by red tide toxins. Marine algal toxins are responsible for >60,000 human toxicity incidents worldwide per

year with a mortality rate of 1.5%, associated with the consumption of contaminated seafood and exposure to aerosols of algal toxins (Bourne et al., 2010). Economic losses in the hotel sector at the county level can reach 15% a month when red tides occur (Bechard, 2019). Therefore, red tides can be harmful to aquatic ecosystems, human health, and the economy. Meanwhile, red tides caused by nontoxic species can also lead to fish kills through oxygen deprivation in the water column as they decay (Xiao et al., 2019). Here we consider blooms as involving cell numbers above a given value, dependent on cell size, as defined in the Methods section (see below). Red tides have a long history, having been recorded in the fossil record, as well as being referenced in the Bible (Anderson, 1997). However, several decades ago red tide algal blooms were infrequent but nowadays wide areas of coastal waters are often impacted by several red tide toxic algal species (Gu et al., 2022; Wang et al., 2023). Reasons for this global expansion of red tides include increased eutrophication, algal transport by ballast water in ships, and the multiple effects of global climate change (Dai et al., 2023; Glibert, 2020).

The recent spread of macroalgal blooms worldwide is causing widespread concern (Bermejo et al., 2023; Lapointe et al., 2021). These extensive seaweed blooms are dominated by the genera *Ulva* and *Sargassum*, which cause green tides and golden tides, respectively (Bermejo et al., 2023). The biggest green tide ever recorded occurred in the Yellow Sea of China in 2009, and covered an area of 2100 km^2 (Xiao et al., 2021). Since 2011, there have been enormous *Sargassum* spp. blooms in the Atlantic Ocean basin causing serious ecological problems and badly affecting tourism (Lapointe et al., 2021). Although bloom-forming macroalgae are not as toxic as red tides, their rapid uptake of nutrients from seawater can cause nutrient limitation for other photosynthetic organisms (Van Alstyne et al., 2015). In addition, hypoxic conditions can be generated by smothering heaps of rotting macroalgal biomass, which is fatal for many marine animals (Young et al., 2022). The poor water quality that results from masses of rotting macroalgae can cause substantial aquaculture losses. For instance, a green tide in China in 2008 caused economic losses of 760–860 million RMB (104–118 million Euros) for just three aquafarms in Shandong province (Ye et al., 2011).

Red tides have a long history in China, and scientific reports date back to 1933 (Liang, 2012). Macroalgal blooms, on the other hand, have only been recorded as occurring over the past two decades in China. At different times, both increasing and decreasing trends of red tides are apparent (Xiao et al., 2019; Zeng et al., 2019). The reasons that drive the changes have been attributed to water quality and warming (Xiao et al., 2019; Zeng et al., 2019). Previous studies have focused on single types (micro or macro) of algal blooms (Bermejo et al., 2023; Dai et al., 2023; Xiao et al., 2019), ignoring their co-evolution and interactions. However, we assume that red tides and macroalgal blooms may interact with each other along with the changing environment. To test this hypothesis, we compiled data on micro- and macroalgal blooms during 1991–2020 and examined long-term patterns in their frequency, distribution, and duration. A tipping point for algal blooms was identified, a correlation of micro- and macroalgal blooms was found and potential drivers were explored. To the best of our knowledge, this is the first study to investigate the interaction between algal blooms and the shift between micro- and macroalgae over a long period, contributing to an understanding of algal bloom trends in the Anthropocene.

2 | MATERIALS AND METHODS

2.1 | Algal bloom data

Data on red tides were acquired from the Bulletin of Chinese Marine Disasters for 1991–2020 issued by the Ministry of Natural Resources of China (former State Oceanic Administration of China) that is publicly available in Chinese (https://www.mnr.gov.cn/sj/sjfw/hy/gbgg/zghyzhgb/), and from the literature (Guo et al., 2015; Li et al., 2023; Liang, 2012; Zhao, 2010). In addition to the overall trends in red tides, the patterns of four main red tide species, *Prorocentrum donghaiense*, *Karenia mikimotoi*, *Noctiluca scintillans*, and *Skeletonema costatum*, which contribute about 70% of red tide occurrences in China, were also analyzed (Li et al., 2023). Systematic monitoring of Harmful Algal Blooms (HABs) has been conducted in China since 1964 following the establishment of China's State Oceanic Administration. There are 34 red tide monitoring areas across the country. The HABs monitoring standard includes four surveys per month during high-risk seasons and one to two surveys per month during other seasons, with surveys every 3 days when harmful algal blooms are expected to occur, and daily monitoring when blooms are detected. The same methods have been used annually within these monitoring areas since 1970 (Xiao et al., 2019). All monitoring tasks included sample collection to determine phytoplankton species density. The occurrence of a bloom is determined to be when cell density exceeds a size-dependent threshold set in the standard procedure, which is $>10^7$, $>10^6$, $>2\times10^5$, $>10^5$, and $>3\times10^3$ cells dm^{-3} for algae with cell lengths of <10, 10–29, 30–99, 100–299, and 300–1000 μm, respectively (HY/T 069-2005). Red tide events that occur outside of the monitoring areas are not included in this study. This may lead to the underestimation of red tide occurrence. However, the monitoring areas cover the coastal waters across China where red tides usually occur, based on historical records. Therefore, the underestimation should be limited and would not impact the variation trend of red tides.

Data on transregional and local green tides were collated from the Bulletin of Chinese Marine Disasters 2008–2020 and the published literature (He et al., 2019; Song et al., 2011; Wei et al., 2011; Xiao et al., 2021; Xing & Hu, 2016; Zeng et al., 2023). Data on golden tides were acquired from Qi et al. (2017), Xing et al. (2017), Ding et al. (2019), Liu, Xia, et al. (2021), Lei et al. (2022), Song, Yan, et al. (2022), and Zheng et al. (2022). After integrating the thresholds in China and abroad, the occurrence of a local green tide is determined to be when coverage exceeds 10,000 m^2 and coverage percentage (the ratio of coverage to distribution) exceeds 1%. Hereafter, 'frequency' means the number of algal outbreaks during a particular

period, 'distribution' is the regional area over which blooms spread, while 'coverage' is the size of the blooms themselves and excludes bloom-free areas in the regional distribution.

2.2 | Environmental data

Nutrient loads from rivers were obtained from Wang et al. (2021) who used an Integrated Model to Assess Global Environment-Global Nutrient Model (IMAGE-GNM) (0.5°×0.5° resolution). Nutrient load from mariculture includes that from fish, prawn, and crab farms. The nutrient load from fish farms was calculated according to Xiong et al. (2022) and that from prawn and crab farms was calculated according to the N and P budget (Ban, 2015). The total nitrogen (TN) and total phosphorus (TP) loads were used to calculate the molar N:P each year for riverine and mariculture inputs. The production of fish, prawns, and crabs was obtained from the China Fishery Statistical Yearbook for the years 1991–2020 (Table S1). The ratios of dissolved silicate (DSi) to dissolved organic nitrogen (DIN) were obtained from Liu et al. (2022) and Zhang et al. (2022). Carbon dioxide data were acquired from China Greenhouse Gas Bulletin for the years 1991–2020, issued by the China Meteorological Administration. Atmospheric CO_2 concentrations were measured at Mount Waliguan, the only station of the World Meteorological Organization/Global Atmosphere Watch in Eurasia. Sea surface temperature (SST) data (1991–2020) were derived from the Met Office Marine Data Bank (Table S2) (http://www.metoffice.gov.uk/hadobs/hadisst/data/download.html), which has a resolution of 1.0°×1.0°. Monitoring data for SST in all 11 coastal administrative areas of China were used to calculate annual means in coastal areas (Table S2).

2.3 | Grazing rate

The grazing pressure on phytoplankton is mainly from microzooplankton that are defined as heterotrophic and mixotrophic organisms with a size range of 20–200 μm. The microzooplankton consists of ciliates, heterotrophic, and mixotrophic dinoflagellates, as well as mesozooplankton nauplii (Liu, Chen, et al., 2021; Sieburth et al., 1978). It has been reported that microzooplankton consume about 59%–75% of daily primary production (Calbet, 2008; Calbet & Landry, 2004). As such, we used their grazing rates to evaluate the top-down controls on phytoplankton by grazers. The microzooplankton grazing rate was estimated using a machine-learning technique known as a Boosted Regression Trees (BRT) model, which has been increasingly used in ecological studies (Elith & Leathwick, 2017). The BRT model was based on a published data set consisting of microzooplankton grazing rate and related environmental parameters in China's marginal seas, including the South China Sea, the East China Sea, and the Yellow Sea (Liu, Chen, et al., 2021). As temperature and Chl *a* concentrations have been reported as the primary factors determining microzooplankton grazing rate, we used them as predictors for the BRT model. The BRT was implemented using the function "gbm.step" in the R package "dismo." The tree complexity was set as 1 and the learning rate was set as 0.001 to allow the model to approach the best performance slowly with more trees to reduce error. Other settings remained as the defaults in "gbm" (Elith & Leathwick, 2017). To evaluate the prediction accuracy of the model, 20% of data from the data set were randomly selected as testing data and excluded from the model fitting. The final fitted BRT models for the training data had 3700 trees, enabling the model to approach the plateau very slowly (Figure S1). The model performs well, and Pearson's correlation coefficient (r) for the model predictions and the testing data is .52 ($p < .001$, Figure S1). We then used this model to predict the microzooplankton grazing rate of each Province in each year (1997–2020). The SST and Chl *a* in all 11 coastal administrative areas of China were input to the model as predictors. SST (Table S2) and Chl *a* (Table S3) data were derived from the Met Office Marine Data Bank and NOAA, respectively. Microzooplankton grazing rate (day^{-1}) in each coastal administrative area (Table S4) was weighed based on their area proportion to calculate annual means. The data after 1997 were presented since Chl *a* data were not monitored before 1997.

2.4 | Statistical analysis

The method used to identify trends in red tide coverage around China followed Ban et al. (2022). We used the Mann–Kendall trend test to analyze whether trends changed significantly ($p < .05$) due to a sustained increasing trend switching abruptly to a decreasing trend, that is, a tipping point.

Linear and nonlinear regressions were used for our time series analysis. Pearson correlations of multiple variables were used to analyze potential relationships between microalgal and macroalgal blooms and the environmental factors including TN, TP, atmospheric CO_2, annual average SST, and grazing rate. Adjusted R-squared was used to avoid the false improvement of the model due to increased independent variables.

3 | RESULTS

Figure 1 shows the widespread distributions of micro- and macroalgal blooms around China in 1991–2020. Red tides have occurred off all coasts of China, with the East China Sea having the highest frequency (58%) and the Yellow Sea having the lowest frequency (10%) during the period 1991–2020. Since 2006, huge transregional green tides occurred in the Yellow Sea while golden tides have affected large areas in the East China Sea and the Yellow Sea. More localized green tides have occurred in coastal waters of the Bohai Sea (Yingkou, Qinhuangdao, Tangshan), the Yellow Sea (Yantai, Nantong), the East China Sea (Ningbo, Xiamen), and the South China Sea (Shantou, Shenzhen, Zhanjiang, Beihai, Lingshui, Sanya) where red tides also occurred.

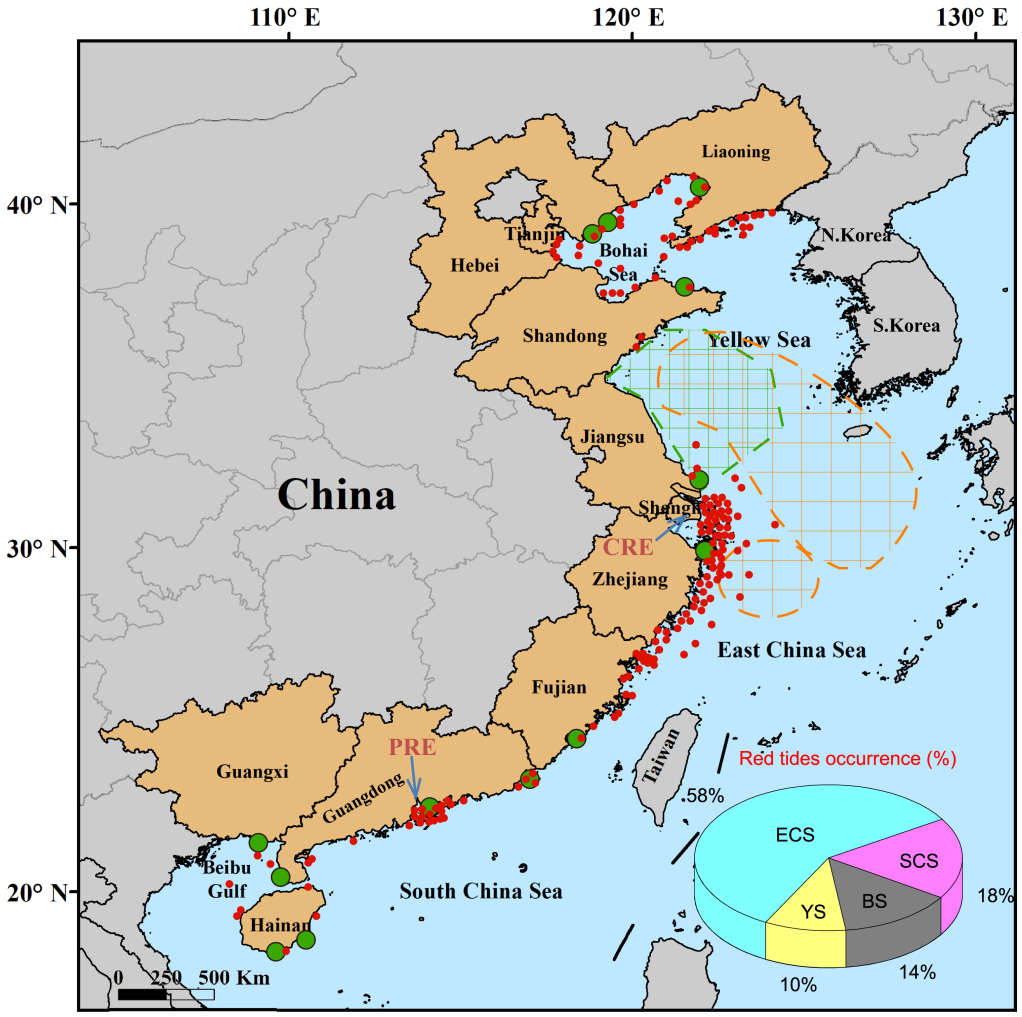

FIGURE 1 Distribution of marine algal blooms around China during 1991–2020. Red and green circles represent localized red and green tides, respectively. Green and brown dashed lines show the extent of very extensive transregional green and golden tides, respectively. The pie chart shows the percentage occurrence of red tides in four seas (BS: Bohai Sea, YS: Yellow Sea, ECS: East China Sea, SCS: South China Sea) during 1991–2020. CRE and PRE represent the Changjiang River estuary and Pearl River estuary, respectively. Map lines delineate study areas and do not necessarily depict accepted national boundaries.

To show more detail on red tides, the distribution of red tides caused by the four main species in China is shown (Figure 2). The occurrence of red tides caused by *Prorocentrum donghaiense* was confined to the coastline of the East China Sea (Figure 2a). *Karenia mikimotoi* dominated red tides also occurred mainly in the coastal waters of the East China Sea but could also be found in the Bohai Sea and the South China Sea (Figure 2b). In contrast, *Noctiluca scintillans* red tides mainly occurred in the Bohai Sea, although they could be detected in the other three seas (the Yellow Sea, the East China Sea, and the South China Sea) (Figure 2c). *Skeletonema costatum* red tides had a relatively even distribution along the coastline of China (Figure 2d) and could be detected in the southernmost location of Hainan province.

The frequency (number of blooms in a given year) of red tides first decreased and then exponentially increased during 1991–2003 ($F_{(3,12)}=92.142$, $p<.001$, $r^2=.907$), with an overall increasing rate of seven times year^{-1} (Figure 3a). After 2003, their frequency decreased yearly until 2020 at a decreasing rate of five times year^{-1} ($F_{(1,16)}=46.825$, $p<.001$, $r^2=.729$). Red tide coverage (Figure 3b) increased by 1896 km^2 year^{-1} during 1991–2005 ($F_{(3,14)}=101.754$, $p<.001$, $r^2=.918$) then decreased by 1687 km^2 year^{-1} from 2005 to 2020 ($F_{(1,14)}=51.204$, $p<.001$, $r^2=.770$). The Mann–Kendall Tau test ($Z=-4.187$, $p<.001$) shows that a tipping point in the trend of red tides occurred in 2005.

No macroalgal blooms were recorded in China until 1999 when transregional green tides started to occur in the Yellow Sea (Figure 3c). Thereafter, the frequency of macroalgal blooms increased linearly ($F_{(1,21)}=596.319$, $p<.001$, $r^2=.964$) and reached 13 blooms per year in 2020. Local green tides have occurred annually since 2003, while transregional golden tides have occurred annually since 2012, stretching across the East China Sea and the Yellow Sea. The increasing frequency of macroalgal blooms with year is mainly due to local green tides because no local golden tides have been reported. When analyzing outbreaks of micro- and macroalgal blooms

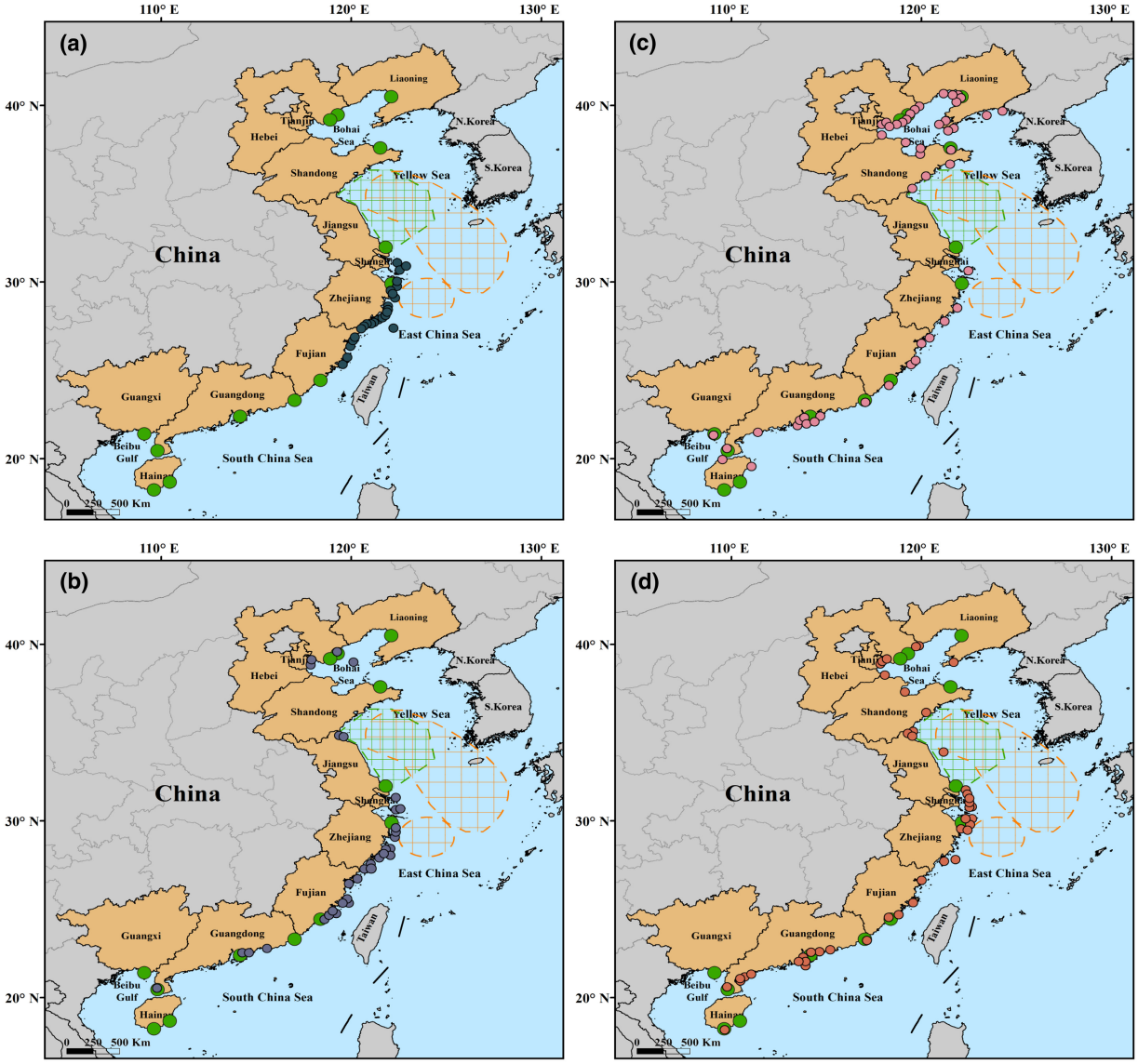

FIGURE 2 Distribution of four types of main red tides along with macroalgal blooms around China during 1991–2020. (a) *Prorocentrum donghaiense* dominant red tides, navy circles; (b) *Karenia mikimotoi* dominant red tides, grey circles; (c) *Noctiluca scintillans* dominant red tides, pink circles; (d) *Skeletonema costatum* dominant red tides, red circles. Green circles represent localized green tides, respectively. Green and brown dashed lines show very extensive transregional green and golden tides, respectively. Map lines delineate study areas and do not necessarily depict accepted national boundaries.

(Figure 3d), a significant negative relationship was found for the frequency between green+golden and red tides during 2005–2020 ($F_{(1,14)}=15.426$, $p=.002<.05$, $r^2=.490$). The increase in the frequency of green+golden tides was accompanied by a decrease in red tide coverage during 2005–2020 ($F_{(1,14)}=42.916$, $p<.001$, $r^2=.736$). These results suggest competition between micro- and macroalgal blooms.

The frequency of red tides caused by the four main species during 1991–2020 was further analyzed (Figure 4). Red tide events caused by *Prorocentrum donghaiense* increased exponentially during 1999–2004 ($F_{(3,13)}=29.286$, $p<.001$, $r^2=.831$), with an overall increase rate of six times year^{-1} (Figure 4a). After 2004, its frequency shows a decreased trend ($F_{(1,15)}=6.211$, $p=.025$, $r^2=.246$). The pattern for *Karenia mikimotoi* is similar to *P. donghaiense* although the decrease after the peak in 2006 was not linear ($F_{(1,13)}=4.298$, $p=.059$, $r^2=.191$, Figure 4b). The frequency of red tides caused by *Noctiluca scintillans* decreased first during 1990–1996 and then increased to a peak in 2003 ($F_{(3,12)}=34.153$, $p<.001$, $r^2=.821$, Figure 4c). Thereafter, it also shows a decreasing trend in spite of large fluctuations ($F_{(1,16)}=3.380$, $p=.085$, $r^2=.123$). In terms of *Skeletonema costatum* (Figure 4d), its red tides increased during 1997–2006 ($F_{(3,15)}=40.468$, $p<.001$, $r^2=.831$) but decreased linearly after that ($F_{(1,13)}=22.803$, $p<.001$, $r^2=.609$). Frequencies of red tides caused by the four species all experienced two stages, with an increase in the first stage but a decrease in the second stage. In the second stage, *S. costatum* had

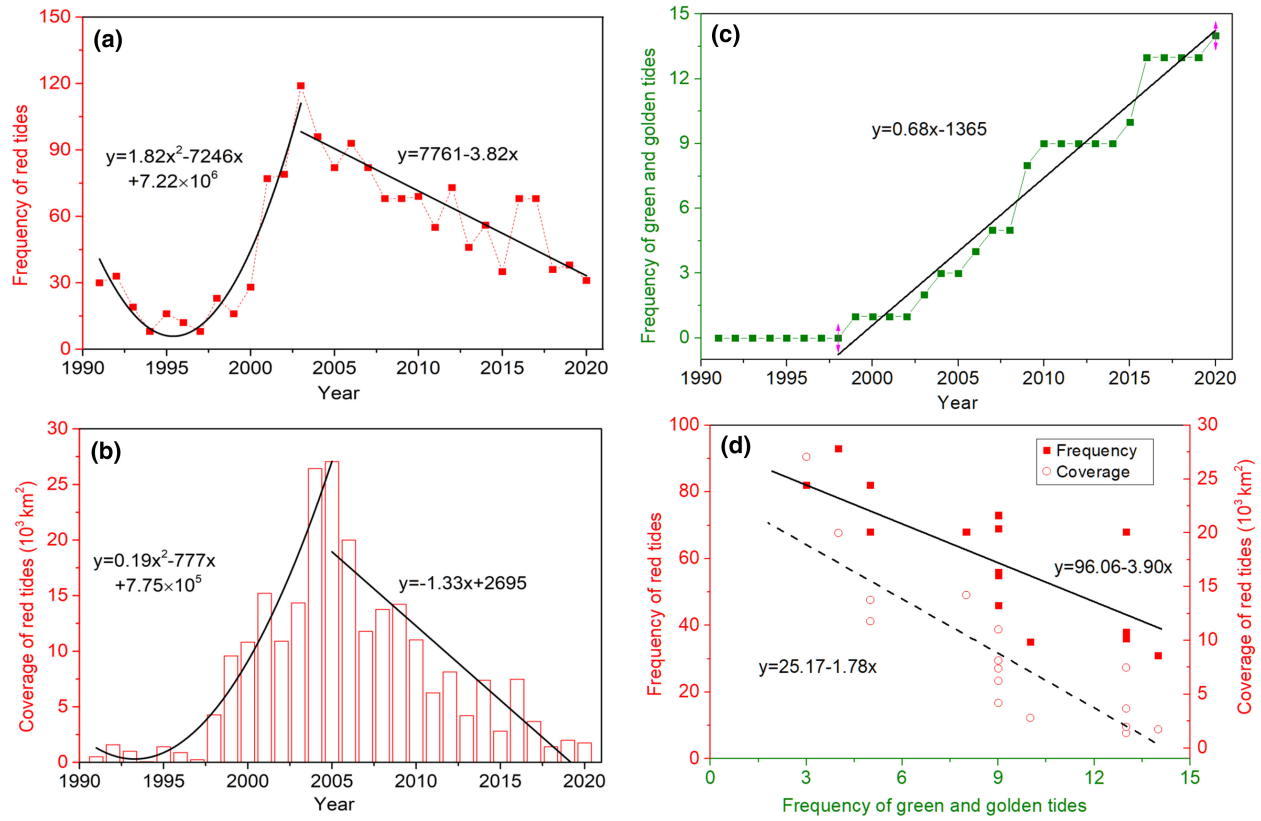

FIGURE 3 Frequency and coverage of red tides and their relationship with macroalgal blooms around China. (a) frequency of red tides; (b) coverage of red tides; (c) frequency of macroalgal blooms; (d) relationships between red tide frequency (filled squares), red tide coverage (open circles) and macroalgal bloom frequency.

the highest rate of decrease while *N. scintillans* had the lowest decrease rate based on the slope values.

The coverage and distribution of green tides in China are shown in Figure 5a. The coverage of green tides during 1999–2007 was small, ranging from 1.83 to 57 km^2. The area affected by green tides increased to a coverage of 653 km^2 in 2008 and then reached a peak of 2103 km^2 in 2009. Afterwards it has since fluctuated between 198 and 793 km^2 during 2010–2020. The regional distribution of green tides was 82 times larger than the coverage of the blooms themselves. Golden tides were first recorded off the Zhejiang coast in the East China Sea in 2012, with a coverage of 33.5 km^2 (Figure 5b). These golden tides had a coverage of 534 km^2 in Chinese waters in 2017 and are now an annual problem, with a coverage of 75.16 km^2 in 2020. The regional distribution of these golden tides was, on average, 1284 times larger than the coverage of the blooms themselves.

Seasonal characteristics of algal bloom occurrences were also analyzed (Figure 5c,d). Red tides have occurred in all months of a year (Figure 5c). May had the highest frequency (442) of red tides in China during 1991–2020, followed by June (334), while December had the lowest frequency (4), followed by November (21). The seasonal pattern of coverage is similar to that of bloom frequency, being highest in May (105,898 km^2) and lowest in December (936 km^2). Unlike red tides, transregional green tides occurred in specific seasons (Figure 5d). They usually began in March or April and ended in July or August. This pattern lasted until September in 2019. Compared to transregional green tides, local green tides had a shorter duration, usually 2–3 months. Due to their wide distribution, from Liaoning province in the North of China to Hainan province in the South of China, the overall duration of all local green tides is very long, with a narrow temporal gap in October and November. Golden tides usually began in March and end in June, but sometimes occur in winter (Figure 5d).

Total nitrogen load discharged from rivers into coastal waters increased from 5.06 Tg in 1991 to 11.03 Tg in 2018 and levelled-off to 10.89 Tg in 2020 (Figure 6a). In contrast, the TN load from mariculture has continued to increase during 1991–2020 and reached 0.33 Tg in 2020 (Figure 6b). The pattern of TP load was similar to TN although that from mariculture had a higher percentage of the total load (0.19%–8.47%) compared to TN (0.03%–2.92%). The N:P ratio of riverine inputs decreased from 30.16 in 1991 to 28.57 in 2020 (Figure 6c). The total N:P (average from all sources) also showed a decreasing trend, from 29.66 in 1991 to 26.94 in 2020. The N:P ratio from mariculture effluents was much lower than that of rivers, fluctuating from 6.80 to 11.28 during 1991–2020. In 2005, when coverage of red algal blooms switched abruptly from an increasing to a decreasing trend, the TN, TP, and N:P ratio were 8.61 Tg $year^{-1}$, 0.76 Tg $year^{-1}$, and 29.15, respectively.

The variation trends of DSi/DIN were also analyzed (Figure 7). The DSi/DIN ratio in the Bohai Sea linearly decreased from 0.59 to

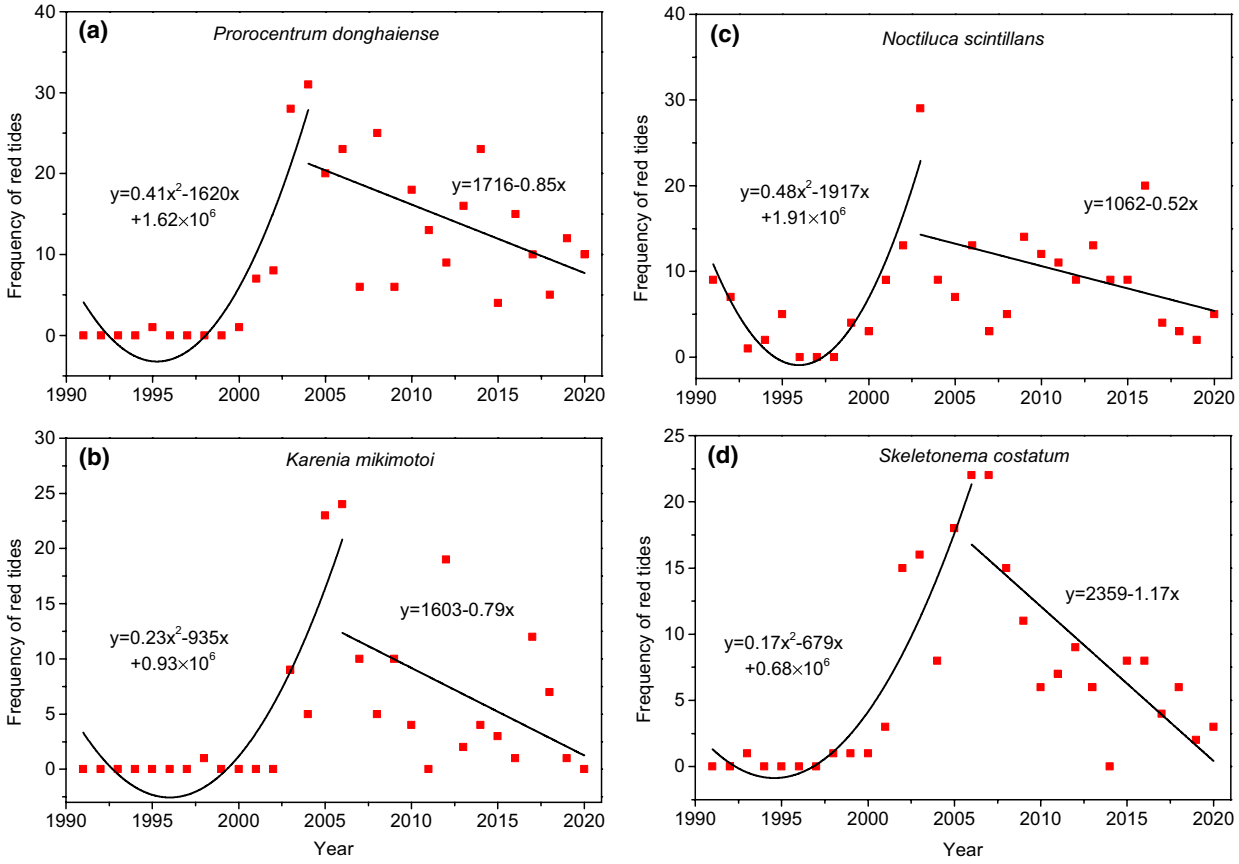

FIGURE 4 Frequency of red tides caused by four main species around China during 1991–2020. (a) *Prorocentrum donghaiense*; (b) *Karenia mikimotoi*; (c) *Noctiluca scintillans*; (d) *Skeletonema costatum*.

0.53 during 2003–2020 ($F_{(1,16)}=7.539$, $p=.014$, $r^2=.278$, Figure 7a). While the DSi/DIN ratio in the Yellow Sea did not show a significant decrease trend ($F_{(1,16)}=0.004$, $p=.951$, $r^2=-.062$, Figure 7b), it decreased from 0.69 in 2003 to 0.64 in 2020 in the Changjiang River estuary ($F_{(1,16)}=8.039$, $p=.012$, $r^2=.293$, Figure 7c) and also decreased from 3.69 in 1990 and to 0.88 in 2016 in the Pearl River estuary ($F_{(1,16)}=50.101$, $p<.001$, $r^2=.743$, Figure 7d). As show in Figure 1, the Changjiang River estuary and Pearl River estuary are two areas that suffer from severe red tides.

Atmospheric CO_2 concentrations increased from 354.7 ± 0.10 ppm in 1991 to 414.53 ± 0.20 ppm in 2020, with a rising rate of 1.99 ppm year^{-1} ($F_{(1,28)}=7637.835$, $p<.001$, $r^2=.996$) and was at 379.7 ± 0.08 ppm when red tide coverage started to decline (Figure 8a). The mean SST for the coastal waters of China during 1991–2020 ($F_{(1,28)}=6.008$, $p=.021$, $r^2=.147$) increased from 18.63°C in 1991 to 19.13°C in 2020, in spite of fluctuations (Figure 8b). The mean SST of all Chinese coastal waters combined was 18.68°C in 2005 when the coverage of red tides started to fall and be replaced by nuisance macroalgal blooms.

In addition to abiotic factors, biotic factors were also analyzed (Figure 9). Chl *a* concentration of coastal waters around China increased from 3.87 in 1997 to 4.83 mg m^{-3} in 2020 ($F_{(1,22)}=15.051$, $p<.001$, $r^2=.379$, Figure 9a). Similar to Chl *a* concentration, zooplankton grazing rate of coastal waters around China also increased from 0.548 to 0.583 day^{-1} during the period of 1997–2020 ($F_{(1,22)}=45.415$, $p<.001$, $r^2=.659$, Figure 9b). The Chl *a* concentration and grazing rate were 3.78 mg m^{-3} and 0.523 day^{-1}, respectively, when the coverage of red tides started to fall.

We used Pearson correlation analysis for multiple variables from 2005 to 2020, the period over which red tides have been diminishing whereas macroalgal blooms have increased (Figure 10). The coverage of red tides had significant negative correlations with the frequency of macroalgal blooms, TN, TP, CO_2, and zooplankton grazing rate ($p<.01$) over this time period. Among them, TN (−0.926) and TP (−0.923) had a very high correlation coefficient with the coverage of red tides, followed by CO_2 (−0.879) and macroalgal blooms (−0.868). *Prorocentrum donghaiense* or *Noctiluca scintillans* did not have significant correlations with biotic or abiotic factors, while *Karenia mikimotoi* (−0.613) and *Skeletonema costatum* (−0.826) had significant negative correlations with the frequency of macroalgal blooms. In contrast, the frequency of macroalgal blooms positively correlated with TN, TP, CO_2, SST, and zooplankton grazing rate ($p<.05$ for SST and $p<.01$ for the others). Among them, CO_2 (0.962), TP (0.955), and TN (0.950) had very high correlation coefficients with the frequency of macroalgal blooms. SST positively correlated with rising atmospheric CO_2 levels at the 0.01 level of statistical significance and with TN and TP at the 0.05 level of statistical significance. Zooplankton grazing rate positively correlated with TN, TP, and CO_2 ($p<.01$).

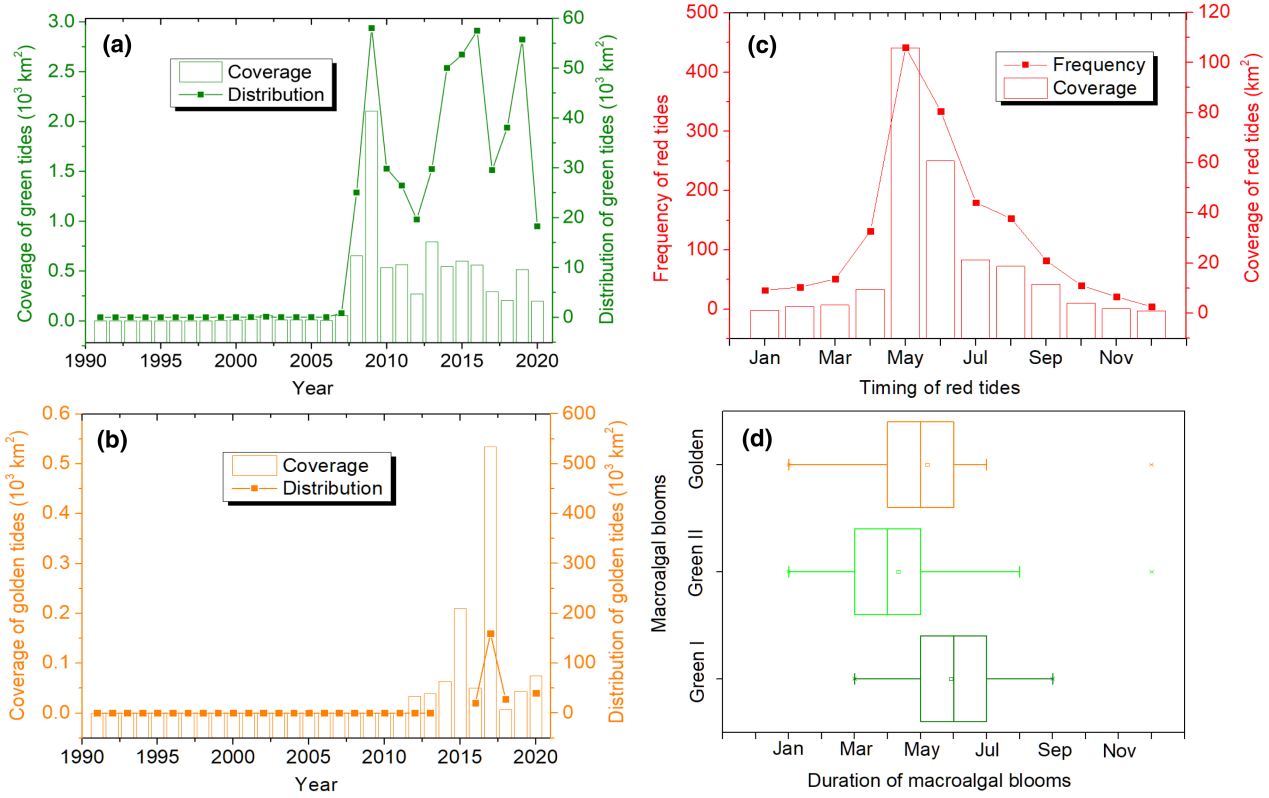

FIGURE 5 All plots based on data from the seas around China from 1991 to 2020; (a) coverage and regional distribution of green and (b) golden tides; (c) seasonal frequency and coverage of red tides; (d) box plots of the timing of macroalgal blooms. Green tides I and II represent transregional and local blooms, respectively. "Distribution" is the regional area over which blooms spread while "coverage" is the actual size of blooms and excludes bloom-free areas in the regional distribution.

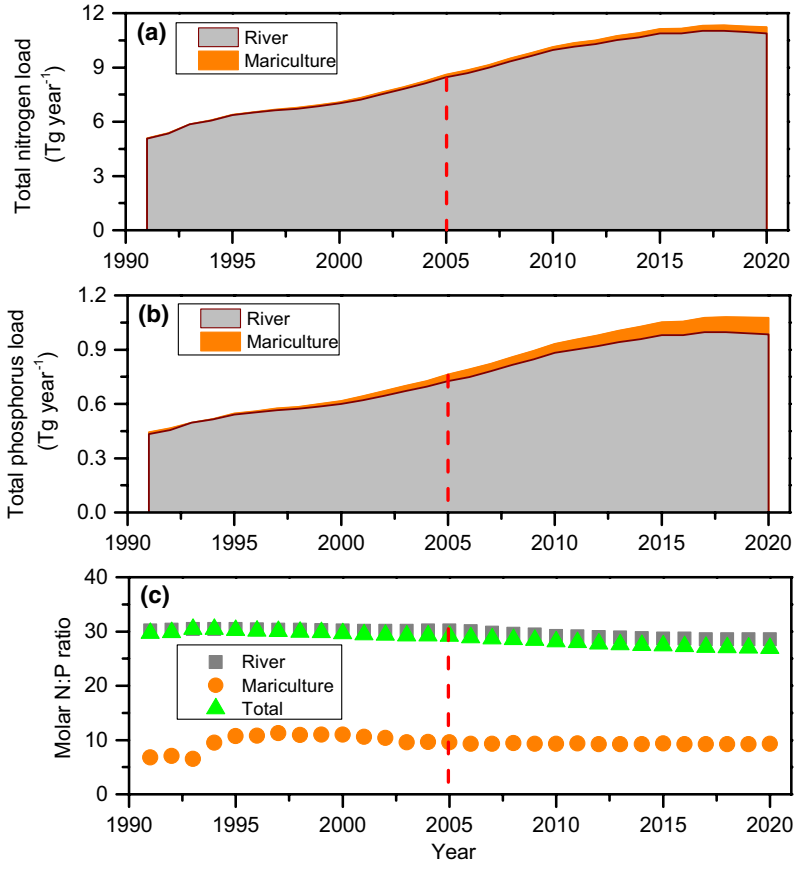

FIGURE 6 Total nitrogen (a) and total phosphorus (b) contributions from riverine and mariculture sources to coastal waters and their ratio (c) around China during 1991–2020. "Total" means the sum of river and mariculture contributions. Red dashed vertical lines indicate the timing of a tipping point in red tides when they started to decrease, following a decade of increasing frequency.

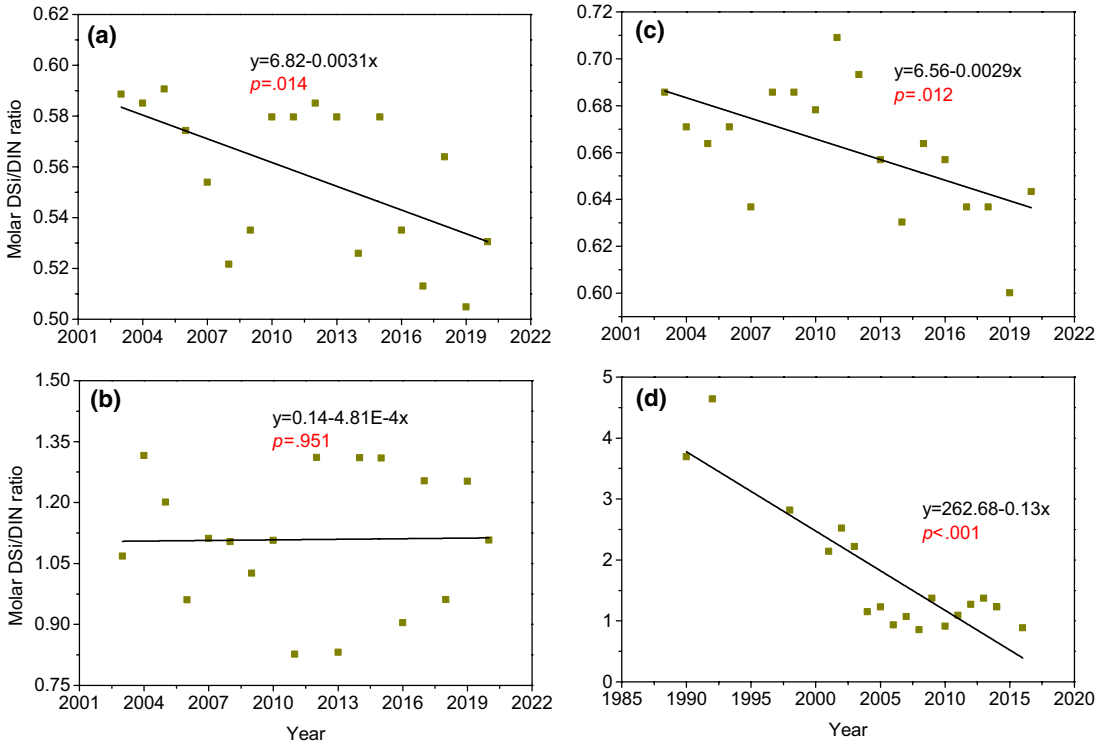

FIGURE 7 Variation of molar DSi/DIN ratios in the Bohai Sea (a), Yellow Sea (b), Changjiang River estuary (c) and Pearl River estuary (d).

FIGURE 8 Mean sea surface temperature of coastal waters around China (a) and atmospheric CO_2 in this region (b) during 1991–2020. Vertical red dashed lines indicate when red tides started to become less frequent.

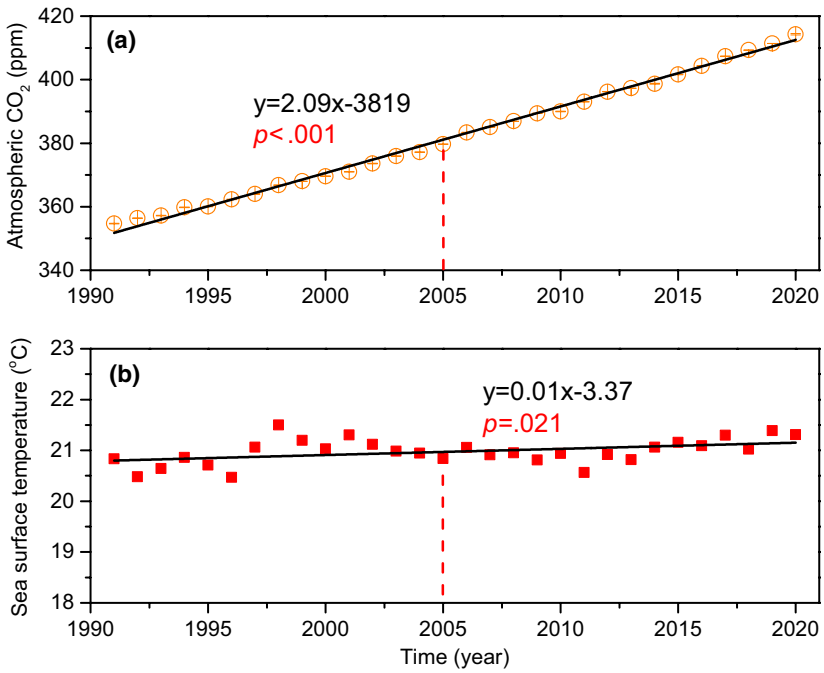

4 | DISCUSSION

4.1 | Trends of red tides and the associated reasons

The frequency of red tides increased rapidly around China during 1995–2003, which has been attributed to the rising discharge of inorganic nutrients from agriculture, sewage, and other land-based sources (Wang et al., 2021). The frequency and coverage of red tides have decreased since 2003 and 2005, respectively, despite a continuing increase in nutrient loads. This decreasing trend was also reported in previous study (He et al., 2021; Sakamoto et al., 2021). A large number of studies have shown that eutrophication and warming can stimulate the occurrence of red tides (Heisler et al., 2008; Xiao et al., 2019). The observed increases in Total Nitrogen, Total

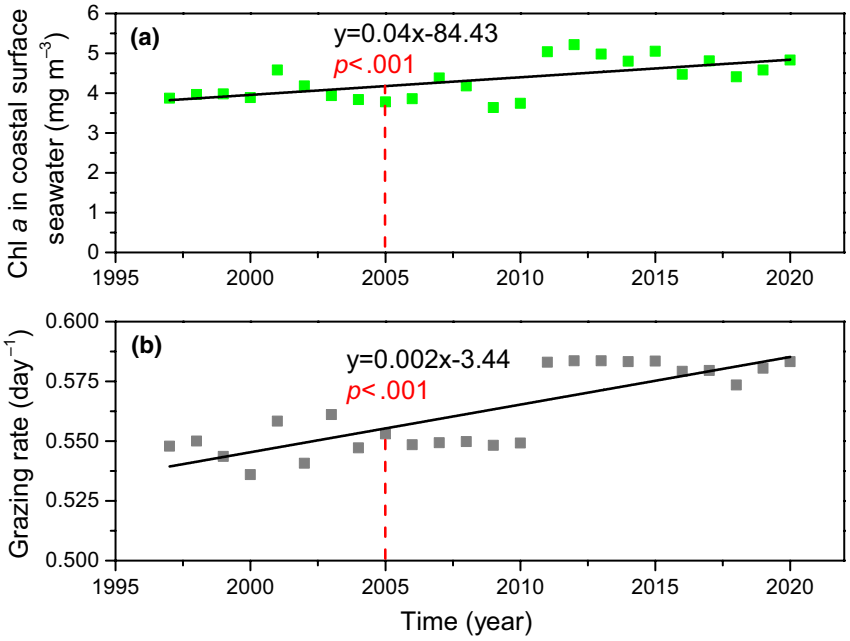

FIGURE 9 Mean Chl *a* concentration (a) and zooplankton grazing rate (b) in coastal waters around China during 1997–2020. Vertical red dashed lines indicate when red tides started to become less frequent.

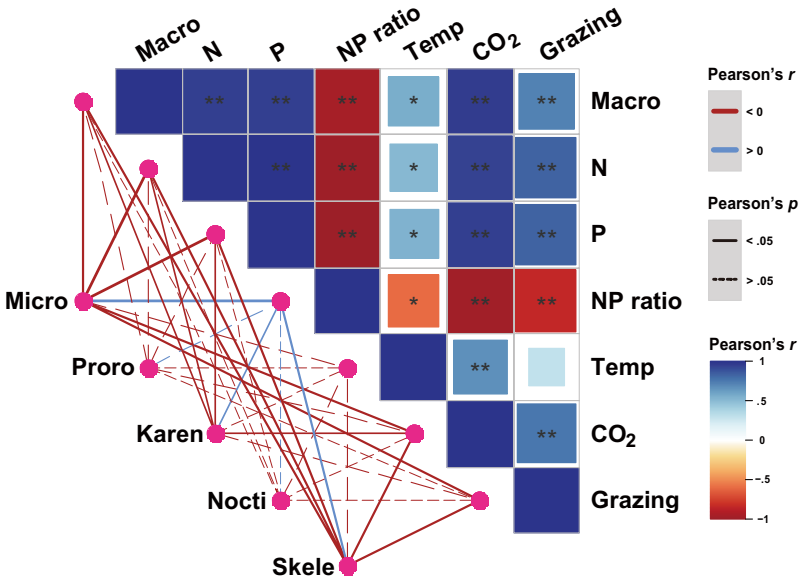

FIGURE 10 Correlation between algal blooms and environmental drivers during 2005–2020. Micro and macro represent coverage of microalgal blooms and frequency of macroalgal blooms, respectively. Frequency rather than coverage of macroalgal blooms was used because coverage could be affected by human intervention (e.g., clean-up removals). Proro, Karen, Nocti and Skele represent *Prorocentrum donghaiense*, *Karenia mikimotoi*, *Noctiluca scintillans* and *Skeletonema costatum* dominated red tides, respectively. "*" and "**" indicate significant correlations at the .05 (two-tailed) and .01 levels (two-tailed), respectively.

Phosphorus, and temperature would not, therefore, be expected to lead to declines in the frequency and coverage of red tides unless some other factor has been driving the negative correlations between red tides and these environmental factors over the past 16 years.

Coverage of red tides was significantly negatively correlated with macroalgal bloom frequency, suggesting that the shrinkage of red tides since 2005 may be caused by increased outbreaks of macroalgal blooms around China, particularly because red tides and green tides overlap in both their distribution and seasonal occurrence. Microalgae and macroalgae are known to compete for nutrients, light, and space in coastal waters (Besterman & Pace, 2018; Gao et al., 2021). Moreover, *Ulva* species (commonly responsible for green tides) can inhibit photosynthesis and growth of red tide microalgae via allelopathic effects (Gao et al., 2019; Sun et al., 2016). The inhibitory effects of *Ulva* species on red tide microalgae have been reported, based on both laboratory and field work (Gao et al., 2019; Imai et al., 2021; Li et al., 2022). The fastest decrease in *S. costatum* dominated red tides may be related to its distribution. Compared to *P. donghaiense* and *K. mikimotoi*, *S. costatum* red tides have a wider distribution, from the southernmost to the northernmost provinces. The wider distribution suggests that there is a greater chance that they would be inhibited by macroalgal blooms. Although *N. scintillans* red tides are also distributed from South to North of China seas, *N. scintillans* is a heterotrophic dinoflagellate that does not compete with *Ulva* and *Sargassum* species for light and inorganic nutrients. Therefore, it is less likely to be inhibited by macroalgal blooms, showing the lowest decrease rate. In addition,

N. scintillans feeds on diatoms and the increased temperature could stimulate its grazing rate and thus growth (McLeod et al., 2012; Sheng et al., 2022). Allelopathic inhibition cannot explain the differential decreases in red tides caused by the four microalgal species since allelochemicals from *U. prolifera* have lower inhibition rates on *S. costatum* compared to *P. donghaiense* (Sun et al., 2019).

4.2 | Trends of macroalgal blooms and the associated reasons

In contrast to the situation with red tides, the frequency of macroalgal blooms has increased each year since they first began around China in 2006. The primary reason for this can be attributed to increases in nutrient load. Large biomass macroalgal blooms require exceptionally high levels of nutrients in the surface seawater. That is a key reason why most macroalgae are restricted to coastal areas where nutrient levels are usually higher than in surface waters of the open ocean. Although microalgae have much higher growth rates than macroalgae under nutrient-limiting conditions, macroalgae can outcompete phytoplankton at high levels of nutrients (Fong & Zedler, 1993; Nan & Dong, 2004). Microalgae can acclimate to nutrient-limiting conditions better than macroalgae because their larger surface area to volume ratio enhances nutrient uptake.

Increased CO_2 may also contribute to outbreaks of macroalgal blooms around China. Carbon dioxide can limit the photosynthesis and growth of algae due to its low concentrations and slow diffusion rates in seawaters (Cornwall et al., 2017; Raven et al., 2017). This limitation is particularly serious for macroalgae and larger microalgae because they have thicker diffusive boundary layers which hinder CO_2 uptake by their cells (Finkel et al., 2010; Noisette & Hurd, 2018). Therefore, macroalgae or larger microalgae could benefit more from increased CO_2 (Wu et al., 2014). However, more dissolved CO_2 leads to ocean acidification, which has a range of effects on seawater carbonate chemistry that can negatively affect some algae (Flynn et al., 2012; Hong et al., 2017; Shi et al., 2019) but stimulate the growth of others, triggering major shifts in coastal algal communities (Cornwall et al., 2017; Harvey et al., 2019). In the coastal waters of China, where chronic and increasing eutrophication has now combined with rising CO_2 levels, blooms of fast-growing and opportunistic macroalgae such as *Ulva* spp. have replaced microalgal red tide blooms, that is, one problem has been replaced by another. In terms of red tide species, it has been reported that CO_2 enrichment increases the maximum population density and carrying capacity of the raphidophyte alga *Heterosigma akashiwo* but decreases these parameters for *S. costatum* (Zheng et al., 2016). Furthermore, growth of *P. donghaiense* is accelerated more strongly than the diatom *Conticribra weissflogii* by simultaneous acidification and eutrophication (Xu et al., 2010). These findings indicate that flagellate algae may be more adaptable to increased acidification and eutrophication than diatoms, which can explain the slower decrease in dinoflagellate red tides in frequency compared to diatom red tides shown in this study.

Temperature may also contribute to the occurrence and expansion of green and golden tides. Compared to many other macroalgae, *Ulva* and *Sargassum* species have higher tolerance to increased temperature (Jiang et al., 2022). While other macroalgae such as kelps may die back due to warming or marine heatwaves (Agostini et al., 2021; Gao et al., 2021; Straub et al., 2019), increased SST can stimulate the growth of *Ulva* and *Sargassum* species (Gao et al., 2017; Sanchez-Rubio et al., 2018). In addition, increased SST can result in the extension of green tides northward, helping to explain the recent occurrence of green tides in the Bohai Sea, an example of coastal ecosystem simplification in the face of multiple stressors (Agostini et al., 2021).

Unlike the continuous increase in the frequency of macroalgal blooms over time, the coverage of macroalgal blooms showed large interannual variability, which could be attributed to human intervention. Since 2016, *Ulva* and *Sargassum* biomass has been collected at the early stages of bloom formation in the Southern Yellow Sea, limiting large-scale proliferation. Since 2019, some measures have also been taken to prevent the outbreak of green tides, such as reducing the densities of *Porphyra* cultivation rafts, and using antifouling chemicals to kill juvenile *Ulva* (Sun et al., 2022). Competition between golden tides and green tides also contributes to annual fluctuations because they overlap in their distribution (Song, Kong, et al., 2022; Song, Yan, et al., 2022). It is also notable that the golden tides are less responsive to eutrophication than green tides and pelagic species of *Sargassum* are known to be adapted to oligotrophic conditions (Devault et al., 2021).

Mean atmospheric CO_2 and SST around China have increased by 140 ppm and around 1.7°C relative to preindustrial levels, respectively (Xiao et al., 2019). This level of warming above preindustrial temperatures already lies within the lower end of five climate tipping point uncertainty ranges (Armstrong McKay et al., 2022). Six climate tipping points, including collapse of the Greenland and West Antarctic ice sheets, die-off of low-latitude coral reefs, and widespread abrupt thawing of permafrost, become likely within the Paris Agreement range of 1.5 to <2°C warming (Armstrong McKay et al., 2022). The present study indicates that it is likely that increased CO_2 and temperature combined with increased nutrient load triggered a tipping point in the coastal seas of China, leading to a shift from microalgal- to macroalgal-dominated eutrophic blooms. Previous laboratory work has also demonstrated that eutrophication combined with increasing CO_2 and temperature can stimulate the settlement, germination, and growth of microscopic propagules of bloom-forming *Ulva* species, suggesting that more intense outbreaks of green tides are likely to become the 'new normal' around Chinese coasts (Gao et al., 2017, 2018). In addition to the environmental factors mentioned above, the expansion of *Porphyra* aquaculture may also contribute to the increased outbreak of floating green tides in the Yellow Sea as the accumulation and disposal of *Ulva prolifera* from *Porphyra* aquaculture rafts is the most likely source of the initial floating biomass (Keesing et al., 2011; Wang et al., 2015).

4.3 | The top-down effects on micro- and macroalgal blooms

In addition to the bottom-up effect, top-down effects may also contribute to the shift of algal blooms. Microzooplankton grazing rate rose with year due mainly to the increased SST and Chl *a* since these two factors can influence grazing rate directly (Liu, Chen, et al., 2021). In addition, our result shows that microzooplankton grazing rate also correlated positively with CO_2 level. This is consistent with the finding of laboratory experiments showing that increased CO_2 stimulated grazing rate of zooplankton (Li & Gao, 2012). The increased grazing rate of zooplankton could contribute to the decreased occurrence and coverage of red tides. The microzooplankton in this study, that consists of ciliates, heterotrophic and mixotrophic dinoflagellates, and mesozooplankton nauplii, can graze any phytoplankton smaller than 200 μm. Their grazing activities are size dependent rather than species dependent (Hansen et al., 1994; Zhou et al., 2015). Therefore, the grazing pressure from microzooplankton may contribute little to the faster decrease in diatom-dominated red tides. In terms of macroalgae, when floating on surface seawater they are inaccessible to benthic grazers and benefit from reduced grazing pressure. Although some epiphytic animals (e.g., gammarid species) feed on floating macroalgae, they only consume a very small proportion of increased biomass of floating macroalgae (Miao et al., 2021; Wang et al., 2020). In addition, the *U. prolifera* fragments resulting from gnawing by *Apohyale* sp. had a higher growth rate than individual thalli, which may lead to higher floating biomass (Miao et al., 2021).

5 | CONCLUSIONS

Increasing eutrophication combined with rising CO_2 and temperature may play an important role as the cause of widespread outbreaks in macroalgal blooms around China since 2006, with warming expanding the northward distribution of these macroalgal blooms. This increased occurrence of macroalgal blooms has been accompanied by a shrinkage of red tides, likely due to competition and inhibition. In addition, increasing grazing rate of microzooplankton also contributes to the decreased frequency and coverage of red tides. While smaller phytoplankton will likely increasingly dominate surface waters of the open ocean, due to warming and increasing nutrient limitation (Falkowski & Oliver, 2007; Gao et al., 2021), this is not the case in coastal areas where people are more directly affected. Around coasts already impacted by eutrophication, due to nutrient inputs from land and mariculture, increasing levels of CO_2 allow macroalgae to compete strongly for resources (Celis-Plá et al., 2015). Macroalgal blooms seem less harmful to human health than microalgal blooms, since they have not been found to excrete toxins. However, the massive biomass of seaweed blooms can have severe impacts on mariculture and tourism and they can produce toxic hydrogen sulfide when decaying, leading to the death of aquatic and terrestrial animals (Smetacek & Zingone, 2013). Thus, monitoring the development of macroalgal tides is needed. In addition, we have to develop strategies to reduce nutrient loads into coastal waters, as well as reducing overall CO_2 emissions. The improvement of agriculture and a more sustainable food system is needed since of nine planetary boundaries (PBs) agriculture is the major driver of four PBs (biosphere integrity, biogeochemical flows, land-system change, and freshwater use) that are in the high or increasing risk zones and a significant driver of climate change (Campbell et al., 2017).

AUTHOR CONTRIBUTIONS

Yuan Feng: Data curation; formal analysis; investigation; software; visualization; writing – review and editing. **Yonglong Xiong:** Data curation; formal analysis; investigation; software; writing – review and editing. **Jason M. Hall-Spencer:** Formal analysis; methodology; validation; visualization; writing – original draft; writing – review and editing. **Kailin Liu:** Data curation; methodology; software; validation; writing – original draft; writing – review and editing. **John Beardall:** Formal analysis; methodology; validation; writing – original draft; writing – review and editing. **Kunshan Gao:** Methodology; resources; validation; writing – review and editing. **Jingke Ge:** Investigation; methodology; writing – review and editing. **Juntian Xu:** Data curation; investigation; validation; writing – review and editing. **Guang Gao:** Conceptualization; data curation; formal analysis; funding acquisition; investigation; methodology; resources; supervision; validation; visualization; writing – original draft; writing – review and editing.

ACKNOWLEDGMENTS

This work was supported by the National Natural Science Foundation of China (42076154), the National Key Research and Development Program of China (2022YFC3105304), and the special fund for Natural Resources Development (Innovation Project of Marine Science and Technology) of Jiangsu Province [grant number JSZRHYKJ202206]. It is a contribution to the Scientific Committee on Oceanic Research (SCOR) Changing Oceans Biological Systems project supported by Royal Society China-UK International Exchanges grant "Effects of ocean acidification and warming in coastal systems" (IEC\NSFC\181187) and by the Japan Society for the Promotion of Science ICONA Program (Grant No: JPJSCCA20210006). We appreciate the kind help from Haifeng Gu from Third Institute of Oceanography, Ministry of Natural Resources, Jianheng Zhang from Shanghai Ocean University, Lijuan Liu from Shandong Marine Resource and Environment Research Institute, Qiang Liu from National Disaster Reduction Centre of China, and Ruobing Wen from Beihai Bureau, Ministry of Natural Resources.

CONFLICT OF INTEREST STATEMENT

The authors declare no competing interests.

DATA AVAILABILITY STATEMENT

The data underpinning the analyses presented here are openly available from Figshare at https://doi.org/10.6084/m9.figshare.24297757 (Feng et al., 2023).

ORCID

Kunshan Gao https://orcid.org/0000-0001-7365-6332
Jingke Ge https://orcid.org/0009-0000-5329-2228
Juntian Xu https://orcid.org/0000-0003-0619-198X
Guang Gao https://orcid.org/0000-0002-9011-9640

REFERENCES

Agostini, S., Harvey, B. P., Milazzo, M., Wada, S., Kon, K., Floc'h, N., Komatsu, K., Kuroyama, M., & Hall-Spencer, J. M. (2021). Simplification, not "tropicalization", of temperate marine ecosystems under ocean warming and acidification. *Global Change Biology*, *27*, 4771–4784. https://doi.org/10.1111/gcb.15749

Anderson, D. M. (1997). Turning back the harmful red tide—Commentary. *Nature*, *388*(6642), 513–514. https://doi.org/10.1038/41415

Anderson, D. M. (2009). Approaches to monitoring, control and management of harmful algal blooms (HABs). *Ocean and Coastal Management*, *52*(7), 342–347. https://doi.org/10.1016/j.ocecoaman.2009.04.006

Armstrong McKay, D. I., Staal, A., Abrams, J. F., Winkelmann, R., Sakschewski, B., Loriani, S., Fetzer, I., Cornell, S. E., Rockstrom, J., & Lenton, T. M. (2022). Exceeding 1.5°C global warming could trigger multiple climate tipping points. *Science*, *377*(6611), eabn7950. https://doi.org/10.1126/science.abn7950

Ban, W. (2015). *Optimization, nitrogen and phosphorus budgets and emergy analysis of different* Portunus trituberculatus *polyculture systems*. (Master dissertation). Ocean University Of China.

Ban, Z., Hu, X., & Li, J. (2022). Tipping points of marine phytoplankton to multiple environmental stressors. *Nature Climate Change*, *12*(11), 1045–1051. https://doi.org/10.1038/s41558-022-01489-0

Bechard, A. (2019). Red tide at morning, tourists take warning? County-level economic effects of HABS on tourism dependent sectors. *Harmful Algae*, *85*, 101689. https://doi.org/10.1016/j.hal.2019.101689

Bermejo, R., Green-Gavrielidis, L., & Gao, G. (2023). Macroalgal blooms in a global change context. *Frontiers in Marine Science*, *10*, 1204117. https://doi.org/10.3389/fmars.2023.1204117

Besterman, A. F., & Pace, M. L. (2018). Do macroalgal mats impact microphytobenthos on mudflats? Evidence from a meta-analysis, comparative survey, and large-scale manipulation. *Estuaries and Coasts*, *41*(8), 2304–2316. https://doi.org/10.1007/s12237-018-0418-3

Bourne, Y., Radic, Z., Araoz, R., Talley, T. T., Benoit, E., Servent, D., Taylor, P., Molgo, J., & Marchot, P. (2010). Structural determinants in phycotoxins and AChBP conferring high affinity binding and nicotinic AChR antagonism. *Proceedings of the National Academy of Sciences of the United States of America*, *107*(13), 6076–6081. https://doi.org/10.1073/pnas.091237210

Calbet, A. (2008). The trophic roles of microzooplankton in marine systems. *ICES Journal of Marine Science*, *3*(65), 325–331. https://doi.org/10.1093/icesjms/fsn013

Calbet, A., & Landry, M. R. (2004). Phytoplankton growth, microzooplankton grazing, and carbon cycling in marine systems. *Limnology and Oceanography*, *49*(1), 51–57. https://doi.org/10.4319/lo.2004.49.1.0051

Campbell, B. M., Beare, D. J., Bennett, E. M., Hall-Spencer, J. M., Ingram, J. S., Jaramillo, F., Ortiz, R., Ramankutty, N., Sayer, J. A., & Shindell, D. (2017). Agriculture production as a major driver of the earth system exceeding planetary boundaries. *Ecology and Society*, *22*(4), 8. https://doi.org/10.5751/ES-09595-220408

Celis-Plá, P. S. M., Hall-Spencer, J. M., Horta, P., Milazzo, M., Korbee, N., Cornwall, C. E., & Figueroa, F. L. (2015). Macroalgal responses to ocean acidification depend on nutrient and light levels. *Frontiers in Marine Science*, *2*, 26. https://doi.org/10.3389/fmars.2015.00026

Cornwall, C. E., Revill, A. T., Hall-Spencer, J. M., Milazzo, M., Raven, J. A., & Hurd, C. L. (2017). Inorganic carbon physiology underpins macroalgal responses to elevated CO_2. *Scientific Reports*, *7*, 46297. https://doi.org/10.1038/srep46297

Dai, Y., Yang, S., Zhao, D., Hu, C., Xu, W., Anderson, D. M., Li, Y., Song, X. P., Boyce, D. G., Gibson, L., Zheng, C., & Feng, L. (2023). Coastal phytoplankton blooms expand and intensify in the 21st century. *Nature*, *615*(7951), 280–284. https://doi.org/10.1038/s41586-023-05760-y

Devault, D. A., Modestin, E., Cottereau, V., Vedie, F., Stiger-Pouvreau, V., Pierre, R., Coynel, A., & Dolique, F. (2021). The silent spring of *Sargassum*. *Environmental Science and Pollution Research*, *28*, 15580–15583. https://doi.org/10.1007/s11356-020-12216-7

Ding, X., Zhang, J., Zhuang, M., Kang, X., Zhao, X., He, P., Liu, S., Liu, J., Wen, Y., & Shen, H. (2019). Growth of *Sargassum horneri* distribution properties of golden tides in the Yangtze Estuary and adjacent waters. *Marine Fisheries*, *42*(2), 188–196. https://doi.org/10.13233/j.cnki.mar.fish.2019.02.007

Elith, J., & Leathwick, J. (2017). *Boosted Regression Trees for ecological modeling*. R documentation. https://cran.r-project.org/web/packages/dismo/vignettes/brt.pdf

Falkowski, P. G., & Oliver, M. J. (2007). Mix and match: How climate selects phytoplankton. *Nature Reviews Microbiology*, *5*(10), 813–819. https://doi.org/10.1038/nrmicro1751

Feng, Y., Xiong, Y., Hall-Spencer, J., Liu, K., Beardall, J., Gao, K., Ge, J., Xu, J., & Gao, G. (2023). Shift in algal blooms from micro- to macroalgae around China with increasing eutrophication and climate change [dataset]. *Figshare*, https://doi.org/10.6084/m9.figshare.24297757

Finkel, Z. V., Beardall, J., Flynn, K. J., Quigg, A., Rees, T. A. V., & Raven, J. A. (2010). Phytoplankton in a changing world: Cell size and elemental stoichiometry. *Journal of Plankton Research*, *32*(1), 119–137. https://doi.org/10.1093/plankt/fbp098

Flynn, K. J., Blackford, J. C., Baird, M. E., Raven, J. A., Clark, D. R., Beardall, J., Brownlee, C., Fabian, H., & Wheeler, G. L. (2012). Changes in pH at the exterior surface of plankton with ocean acidification. *Nature Climate Change*, *2*(10), 510–513. https://doi.org/10.1038/nclimate1489

Fong, P., & Zedler, J. B. (1993). Temperature and light effects on the seasonal succession of algal communities in shallow coastal lagoons. *Journal of Experimental Marine Biology and Ecology*, *171*(2), 259–272. https://doi.org/10.1016/0022-0981(93)90008-C

Gao, G., Clare, A. S., Rose, C., & Caldwell, G. S. (2017). Eutrophication and warming-driven green tides (*Ulva rigida*) are predicted to increase under future climate change scenarios. *Marine Pollution Bulletin*, *114*(1), 439–447. https://doi.org/10.1016/j.marpolbul.2016.10.003

Gao, G., Clare, A. S., Rose, C., & Caldwell, G. S. (2018). *Ulva rigida* in the future ocean: Potential for carbon capture, bioremediation and biomethane production. *GCB Bioenergy*, *10*(1), 39–51. https://doi.org/10.1111/gcbb.12465

Gao, G., Fu, Q., Beardall, J., Wu, M., & Xu, J. (2019). Combination of ocean acidification and warming enhances the competitive advantage of *Skeletonema costatum* over a green tide alga, *Ulva linza*. *Harmful Algae*, *85*, 101698. https://doi.org/10.1016/j.hal.2019.101698

Gao, G., Zhao, X., Jiang, M., & Gao, L. (2021). Impacts of marine heatwaves on algal structure and carbon sequestration in conjunction with ocean warming and acidification. *Frontiers in Marine Science*, *8*, 758651. https://doi.org/10.3389/fmars.2021.758651

Glibert, P. M. (2020). Harmful algae at the complex nexus of eutrophication and climate change. *Harmful Algae*, *91*, 101583. https://doi.org/10.1016/j.hal.2019.03.001

Gu, H., Wu, Y., Lü, S., Lu, D., Tang, Y. Z., & Qi, Y. (2022). Emerging harmful algal bloom species over the last four decades in China. *Harmful Algae*, *111*, 102059. https://doi.org/10.1016/j.hal.2021.102059

Guo, H., Ding, D. W., Lin, F. A., & Guan, C. J. (2015). Characteristics and patterns of red tide in China coastal waters during the last 20a. *Advances in Marine Science*, *33*(4), 547–558.

Hallegraeff, G. M. (2010). Ocean climate change, phytoplankton community responses, and harmful algal blooms: A formidable predictive challenge. *Journal of Phycology*, *46*(2), 220–235. https://doi.org/10.1111/j.1529-8817.2010.00815.x

Hansen, B., Bjornsen, P. K., & Hansen, P. J. (1994). The size ratio between planktonic predators and their prey. *Limnology and Oceanography*, *39*(2), 395–403. https://doi.org/10.4319/lo.1994.39.2.0395

Harvey, B. P., Agostini, S., Kon, K., Wada, S., & Hall-Spencer, J. M. (2019). Diatoms dominate and alter marine food-webs when CO_2 rises. *Diversity*, *11*(12), 242. https://doi.org/10.3390/d11120242

He, P., Zhang, J., Huo, Y., & Cai, C. (2019). *Green tides of China*. Science Press.

He, X., Chen, C., Lu, C., Wang, L., & Chen, H. (2021). Spatial-temporal distribution of red tide in coastal China. *IOP Conference Series: Earth and Environmental Science*, *783*, 012141. https://doi.org/10.1088/1755-1315/783/1/012141

Heisler, J., Glibert, P. M., Burkholder, J. M., Anderson, D. M., Cochlan, W., Dennison, W. C., Gobler, C., Dortch, Q., Heil, C., Humphries, E., Lewitus, A., Magnien, R., Marshall, H., Sellner, K., Stockwell, D., Stoecker, D., & Suddleson, M. (2008). Eutrophication and harmful algal blooms: A scientific consensus. *Harmful Algae*, *8*(1), 3–13. https://doi.org/10.1016/j.hal.2008.08.006

Hong, H., Shen, R., Zhang, F., Wen, Z., Chang, S., Lin, W., Kranz, S. A., Luo, Y. W., Kao, S. J., Morel, F. M. M., & Shi, D. (2017). The complex effects of ocean acidification on the prominent N_2-fixing cyanobacterium *Trichodesmium*. *Science*, *356*(6337), 527–531. https://doi.org/10.1126/science.aal2981

Imai, I., Inaba, N., & Yamamoto, K. (2021). Harmful algal blooms and environmentally friendly control strategies in Japan. *Fisheries Science*, *87*(4), 437–464. https://doi.org/10.1007/s12562-021-01524-7

Jiang, M., Gao, L., Huang, R., Lin, X., & Gao, G. (2022). Differential responses of bloom-forming *Ulva intestinalis* and economically important *Gracilariopsis lemaneiformis* to marine heatwaves under changing nitrate conditions. *Science of the Total Environment*, *840*, 156591. https://doi.org/10.1016/j.scitotenv.2022.156591

Keesing, J. K., Liu, D., Fearns, P., & Garcia, R. (2011). Inter-and intra-annual patterns of *Ulva prolifera* green tides in the Yellow Sea during 2007–2009, their origin and relationship to the expansion of coastal seaweed aquaculture in China. *Marine Pollution Bulletin*, *62*(6), 1169–1182. https://doi.org/10.1016/j.marpolbul.2011.03.040

Lapointe, B. E., Brewton, R. A., Herren, L. W., Wang, M., Hu, C., McGillicuddy, D. J., Jr., Lindell, S., Hernandez, F. J., & Morton, P. L. (2021). Nutrient content and stoichiometry of pelagic *Sargassum* reflects increasing nitrogen availability in the Atlantic Basin. *Nature Communications*, *12*(1), 3060. https://doi.org/10.1038/s41467-021-23135-7

Lei, X., Zhang, Y., Jiang, L., Luo, Y., Zhou, G., Sun, Y., & Huang, H. (2022). Zonal macroalgae blooms influenced by different aquaculture discharges in the Xuwen fringing reef, southern China. *Science of the Total Environment*, *822*, 153594. https://doi.org/10.1016/j.scitotenv.2022.153594

Li, D., Gao, Z., & Wang, Y. (2022). Research on the long-term relationship between green tide and chlorophyll-*a* concentration in the Yellow Sea based on Google Earth Engine. *Marine Pollution Bulletin*, *177*, 113574. https://doi.org/10.1016/j.marpolbul.2022.113574

Li, W., & Gao, K. (2012). A marine secondary producer respires and feeds more in a high CO_2 ocean. *Marine Pollution Bulletin*, *64*(4), 699–703.

Li, Z., Zuo, X., & Teng, J. (2023). GIS-based temporal and spatial patterns of red tides in the coastal waters of China from 1950 to 2020. *Acta Scientiae Circumstantiae*, *43*(6), 203–214. https://doi.org/10.13671/j.hjkxxb.2022.0403

Liang, Y. (2012). *Investigation and evaluation of red tide disaster in China (1933–2009)*. China Ocean Press.

Liu, H., Lin, L., Wang, Y., Du, L., Wang, S., Zhou, P., Yu, Y., Gong, X., & Lu, X. (2022). Reconstruction of monthly surface nutrient concentrations in the Yellow and Bohai Seas from 2003–2019 using machine learning. *Remote Sensing*, *14*(19), 5021. https://doi.org/10.3390/rs14195021

Liu, J., Xia, J., Zhuang, M., Zhang, J., Sun, Y., Tong, Y., Zhao, S., & He, P. (2021). Golden seaweed tides accumulated in *Pyropia* aquaculture areas are becoming a normal phenomenon in the Yellow Sea of China. *Science of the Total Environment*, *774*, 145726. https://doi.org/10.1016/j.scitotenv.2021.145726

Liu, K., Chen, B., Zheng, L., Su, S., Huang, B., Chen, M., & Liu, H. (2021). What controls microzooplankton biomass and herbivory rate across marginal seas of China? *Limnology and Oceanography*, *66*(1), 61–75. https://doi.org/10.1002/lno.11588

McLeod, D. J., Hallegraeff, G. M., Hosie, G. W., & Richardson, A. J. (2012). Climate-driven range expansion of the red-tide dinoflagellate *Noctiluca scintillans* into the Southern Ocean. *Journal of Plankton Research*, *34*(4), 332–337. https://doi.org/10.1093/plankt/fbr112

Miao, X., Xiao, J., Fan, S., Zang, Y., Zhang, X., & Wang, Z. (2021). Assessing herbivorous impacts of *Apohyale* sp. on the *Ulva prolifera* Green tide in China. *Frontiers in Plant Science*, *12*, 795560. https://doi.org/10.3389/fpls.2021.795560

Nan, C., & Dong, S. (2004). Comparative studies on phosphorus uptake and growth kinetics of the microalga *Tetraselmis subcordiformis* and the macroalga *Ulva pertusa*. *Journal of Ocean University of China*, *3*(1), 56–59. https://doi.org/10.1007/s11802-004-0009-8

Noisette, F., & Hurd, C. (2018). Abiotic and biotic interactions in the diffusive boundary layer of kelp blades create a potential refuge from ocean acidification. *Functional Ecology*, *32*(5), 1329–1342. https://doi.org/10.1111/1365-2435.13067

Qi, L., Hu, C., Wang, M., Shang, S., & Wilson, C. (2017). Floating algae blooms in the East China Sea. *Geophysical Research Letters*, *44*(22), 11501–11509. https://doi.org/10.1002/2017GL075525

Raven, J. A., Beardall, J., & Sanchez-Baracaldo, P. (2017). The possible evolution and future of CO_2-concentrating mechanisms. *Journal of Experimental Botany*, *68*(14), 3701–3716. https://doi.org/10.1093/jxb/erx110

Sakamoto, S., Lim, W. A., Lu, D., Dai, X., Orlova, T., & Iwataki, M. (2021). Harmful algal blooms and associated fisheries damage in East Asia: Current status and trends in China, Japan, Korea and Russia. *Harmful Algae*, *102*, 101787. https://doi.org/10.1016/j.hal.2020.101787

Sanchez-Rubio, G., Perry, H., Franks, J. S., & Johnson, D. R. (2018). Occurrence of pelagic *Sargassum* in waters of the US Gulf of Mexico in response to weather-related hydrographic regimes associated with decadal and interannual variability in global climate. *Fishery Bulletin*, *116*(1), 93–106. https://doi.org/10.7755/FB.116.1.10

Sheng, L., Jiang, Z., Sun, Z., Zhu, Y., Zhai, H., Ding, L., Tong, M., Chen, J., Chen, Q., & Zeng, J. (2022). *Noctiluca Scintillans* distribution largely regulated by phytoplankton biomass in the East China Sea and Southern Yellow Sea. *Frontiers in Marine Science*, *9*, 899334. https://doi.org/10.3389/fmars.2022.899334

Shi, D., Hong, H., Su, X., Liao, L., Chang, S., & Lin, W. (2019). The physiological response of marine diatoms to ocean acidification: Differential roles of seawater pCO_2 and pH. *Journal of Phycology*, *55*(3), 521–533. https://doi.org/10.1111/jpy.12855

Sieburth, J. M., Smetácek, V., & Lenz, J. (1978). Pelagic ecosystem structure: Heterotrophic compartments of the plankton and their relationship to plankton size fractions. *Limnology and Oceanography*, *23*, 1256–1263. https://doi.org/10.4319/lo.1978.23.6.1256

Smetacek, V., & Zingone, A. (2013). Green and golden seaweed tides on the rise. *Nature*, *504*(7478), 84–88. https://doi.org/10.1038/nature12860

Song, M., Kong, F., Li, Y., Zhao, J., Yu, R., Zhou, M., Jiang, P., & Yan, T. (2022). A massive green tide in the Yellow Sea in 2021: Field investigation and analysis. *International Journal of Environmental Research and Public Health*, *19*(18), 11753. https://doi.org/10.3390/ijerph191811753

Song, M., Yan, T., Kong, F., Wang, Y., & Zhou, M. (2022). Increased diversity and environmental threat of harmful algal blooms in the

Southern Yellow Sea, China. *Journal of Oceanology and Limnology*, *40*(6), 2107–2119. https://doi.org/10.1007/s00343-021-1209-4

Song, X., Sun, G., Zhang, X., Ma, Y., Ren, L., Jiang, X., & Wang, W. (2011). Likely causes of *Enteromorpha linza* green tide and its effect on the environmental factors in Yantai Cop Bay. *Journal of Safety and Environment*, *11*(3), 151–156.

Straub, S. C., Wernberg, T., Thomsen, M. S., Moore, P. J., Burrows, M. T., Harvey, B. P., & Smale, D. A. (2019). Resistance, extinction, and everything in between—The diverse responses of seaweeds to marine heatwaves. *Frontiers in Marine Science*, *6*, 763. https://doi.org/10.3389/fmars.2019.00763

Sun, Y., Dong, S., Guo, G., Guo, L., & Pu, Y. (2019). Antialgal activity of glycoglycerolipids derived from a green macroalgae *Ulva prolifera* on six species of red tide microalgae. *IOP Conference Series: Materials Science and Engineering*, *484*(1), 012057. https://doi.org/10.1088/1757-899X/484/1/012057

Sun, Y., Wang, H., Guo, G., Pu, Y., Yan, B., & Wang, C. (2016). Isolation, purification, and identification of antialgal substances in green alga *Ulva prolifera* for antialgal activity against the common harmful red tide microalgae. *Environmental Science and Pollution Research*, *23*(2), 1449–1459. https://doi.org/10.1007/s11356-015-5377-7

Sun, Y., Xia, Z., Cao, X., Tong, Y., He, R., Fu, M., Sun, J., Xu, H., Xia, J., Liu, J., & Kim, J. K. (2022). A mixed acid treatment for the prevention of *Ulva prolifera* attachment to *Neopyropia* aquaculture rafts: Laboratory experimentation. *Marine Pollution Bulletin*, *184*, 114134. https://doi.org/10.1016/j.marpolbul.2022.114134

Van Alstyne, K. L., Nelson, T. A., & Ridgway, R. L. (2015). Environmental chemistry and chemical ecology of "Green tide" seaweed blooms. *Integrative and Comparative Biology*, *55*(3), 518–532. https://doi.org/10.1093/icb/icv035

Wang, G., Wang, H., Gao, S., Huan, L., Wang, X. L., Gu, W. H., Xie, X.-J., Zhang, J.-H., Sun, S., Yu, R.-C., He, P.-M., Zheng, Z.-B., Lin, A.-P., Niu, J.-F., Wang, L.-J., Zhang, B.-Y., Shen, S.-D., & Lu, S. (2020). Study on the biological mechanism of green tide. *Oceanologia et Limnologia Sinica*, *51*(4), 789–808. https://doi.org/10.11693/hyhz20200300078

Wang, H., Bouwman, A. F., Van Gils, J., Vilmin, L., Beusen, A. H., Wang, J., Liu, X., Yu, Z., & Ran, X. (2023). Hindcasting harmful algal bloom risk due to land-based nutrient pollution in the eastern Chinese coastal seas. *Water Research*, *231*, 119669. https://doi.org/10.1016/j.watres.2023.119669

Wang, J., Bouwman, A. F., Liu, X., Beusen, A. H. W., Van Dingenen, R., Dentener, F., Yao, Y., Glibert, P. M., Ran, X., Yao, Q., Xu, B., Yu, R., Middelburg, J. J., & Yu, Z. (2021). Harmful algal blooms in Chinese coastal waters will persist due to perturbed nutrient ratios. *Environmental Science & Technology Letters*, *8*(3), 276–284. https://doi.org/10.1021/acs.estlett.1c00012

Wang, Z., Xiao, J., Fan, S., Li, Y., Liu, X., & Liu, D. (2015). Who made the world's largest green tide in China?—An integrated study on the initiation and early development of the green tide in Yellow Sea. *Limnology and Oceanography*, *60*(4), 1105–1117. https://doi.org/10.1002/lno.10083

Wei, W., Du, H., Jiang, P., Lin, X., Cai, D., & Ding, L. (2011). *Overview of the first green tide outbreak in the Nan'ao sea area of eastern Guangdong in 2011*. Collection of Abstracts of the Eighth Member Congress and Sixteenth Academic Symposium of the Chinese Psychological Society.

Wu, Y., Campbell, D. A., Irwin, A. J., Suggett, D. J., & Finkel, Z. V. (2014). Ocean acidification enhances the growth rate of larger diatoms. *Limnology and Oceanography*, *59*(3), 1027–1034. https://doi.org/10.4319/lo.2014.59.3.1027

Xiao, J., Wang, Z., Liu, D., Fu, M., Yuan, C., & Yan, T. (2021). Harmful macroalgal blooms (HMBs) in China's coastal water: Green and golden tides. *Harmful Algae*, *107*, 102061. https://doi.org/10.1016/j.hal.2021.102061

Xiao, X., Agusti, S., Pan, Y., Yu, Y., Wu, J., & Duarte, C. M. (2019). Warming amplifies the frequency of harmful algal blooms with eutrophication in Chinese coastal waters. *Environmental Science & Technology*, *53*(22), 13031–13041. https://doi.org/10.1021/acs.est.9b03726

Xing, Q., Guo, R., Wu, L., An, D., Cong, M., Qin, S., & Li, X. (2017). High-resolution satellite observations of a new hazard of golden tides caused by floating *Sargassum* in winter in the Yellow Sea. *IEEE Geoscience and Remote Sensing Letters*, *14*(10), 1815–1819. https://doi.org/10.1109/LGRS.2017.2737079

Xing, Q., & Hu, C. (2016). Mapping macroalgal blooms in the Yellow Sea and East China Sea using HJ-1 and Landsat data: Application of a virtual baseline reflectance height technique. *Remote Sensing of Environment*, *178*, 113–126. https://doi.org/10.1016/j.rse.2016.02.065

Xiong, Y., Gao, L., Qu, L., Xu, J., Ma, Z., & Gao, G. (2022). The contribution of fish and seaweed mariculture to the coastal fluxes of biogenic elements in two important aquaculture areas, China. *Science of the Total Environment*, *856*, 159056. https://doi.org/10.1016/j.scitotenv.2022.159056

Xu, D., Zhou, B., Wang, Y., Ju, Q., Yu, Q., & Tang, X. (2010). Effect of CO_2 enrichment on competition between *Skeletonema costatum* and *Heterosigma akashiwo*. *Chinese Journal of Oceanology and Limnology*, *28*, 933–939. https://doi.org/10.1007/s00343-010-9071-9

Ye, N., Zhang, X., Mao, Y., Liang, C., Xu, D., Zou, J., Zhuang, Z., & Wang, Q. (2011). Green tides' are overwhelming the coastline of our blue planet: Taking the world's largest example. *Ecological Research*, *26*(3), 477–485. https://doi.org/10.1007/s11284-011-0821-8

Young, C. S., Lee, C. S., Sylvers, L. H., Venkatesan, A. K., & Gobler, C. J. (2022). The invasive red seaweed, *Dasysiphonia japonica*, forms harmful algal blooms: Mortality in early life stage fish and bivalves and identification of putative toxins. *Harmful Algae*, *118*, 102294. https://doi.org/10.1016/j.hal.2022.102294

Zeng, B., Sun, Y., Song, W., Wang, Z., & Zhang, X. (2023). Recurrence of the green tide in the Bohai Sea, China: A green tide caused by coastal reclamation projects. *Journal of Sea Research*, *191*, 102333. https://doi.org/10.1016/j.seares.2022.102333

Zeng, J., Yin, B., Wang, Y., & Huai, B. (2019). Significantly decreasing harmful algal blooms in China seas in the early 21st century. *Marine Pollution Bulletin*, *139*, 270–274. https://doi.org/10.1016/j.marpolbul.2019.01.002

Zhang, L., Yang, Y., He, W., Xu, J., & Li, R. (2022). Fluxes of riverine nutrient to the Zhujiang River estuary and its potential eutrophication effect. *Acta Oceanologica Sinica*, *41*(6), 88–98. https://doi.org/10.1007/s13131-021-1919-7

Zhao, D. (2010). *Occurrence regularity of red tide disaster in typical sea areas of China*. China Ocean Press.

Zheng, F., Tu, T., Liu, F., Huang, X., & Li, S. (2016). Influence of acidification and eutrophication on physiological functions of *Conticribra weissflogii* and *Prorocentrum donghaiense*. *Aquatic Toxicology*, *181*, 11–21. https://doi.org/10.1016/j.aquatox.2016.10.024

Zheng, L., Wu, M., Zhao, J., Wang, D., Zhou, M., & Zhao, L. (2022). Remote sensing monitoring and temporal and spatial distribution characteristics of gold tide in the South Yellow Sea. *Haiyang Xuebao*, *44*(5), 12–24. https://doi.org/10.12284/hyxb2022095

Zhou, L., Tan, Y., Huang, L., Hu, Z., & Ke, Z. (2015). Seasonal and size-dependent variations in the phytoplankton growth and microzooplankton grazing in the southern South China Sea under the influence of the east Asian monsoon. *Biogeosciences*, *12*(22), 6809–6822. https://doi.org/10.5194/bg-12-6809-2015

DATA SOURCES

Ban, W. (2015b). *Optimization, nitrogen and phosphorus budgets and emergy analysis of different* Portunus trituberculatus *polyculture systems*. (Master dissertation). Ocean University Of China.

Bulletin of Chinese Marine Disasters. https://www.mnr.gov.cn/sj/sjfw/hy/gbgg/zghyzhgb/

Cao, Y., Guo, Y., Li, P., Gao, Y., Chen, L., & Chen, F. (2016). Study on green tide plant *Enteromorpha* occurred at inshore in the Jimei, Xiamen. *Journal of Jimei University (Natural Science)*, *21*(2), 94–98.

China Fishery Statistical Yearbook. https://www.zgtjnj.org/search.aspx?key=%E4%B8%AD%E5%9B%BD%E6%B8%94%E4%B8%9A%E7%BB%9F%E8%AE%A1%E5%B9%B4%E9%89%B4

China Greenhouse Gas Bulletin. https://data.cma.cn/data/cdcdetail/dataCode/G.0029.0001.S001.html

Ding, X., Zhang, J., Zhuang, M., Kang, X., Zhao, X., He, P., Liu, S., Liu, J., Wen, Y., & Shen, H. (2019b). Growth of *Sargassum horneri* distribution properties of golden tides in the Yangtze estuary and adjacent waters. *Marine Fisheries*, *42*(2), 188–196. https://doi.org/10.13233/j.cnki.mar.fish.2019.02.007

Guo, H., Ding, D. W., Lin, F. A., & Guan, C. J. (2015b). Characteristics and patterns of red tide in China coastal waters during the last 20a. *Advances in Marine Science*, *33*(4), 547–558.

Han, X., Kuang, C., Li, Y., Song, W., Qin, R., & Wang, D. (2022). Numerical modeling of a green tide migration process with multiple artificial structures in the western Bohai Sea, China. *Applied Sciences*, *12*(6), 3017.

He, P., Zhang, J., Huo, Y., & Cai, C. (2019b). *Green tides of China*. Science Press.

Hu, C., Li, D., Chen, C., Ge, J., Muller-Karger, F. E., Liu, J., Yu, F., & He, M. X. (2010). On the recurrent *Ulva prolifera* blooms in the Yellow Sea and East China Sea. *Journal of Geophysical Research: Oceans*, *115*, C05017. https://doi.org/10.1029/2009JC005561

Lei, X., Zhang, Y., Jiang, L., Luo, Y., Zhou, G., Sun, Y., & Huang, H. (2022b). Zonal macroalgae blooms influenced by different aquaculture discharges in the Xuwen fringing reef, southern China. *Science of the Total Environment*, *822*, 153594. https://doi.org/10.1016/j.scitotenv.2022.153594

Li, Z., Zuo, X., & Teng, J. (2023b). GIS-based temporal and spatial patterns of red tides in the coastal waters of China from 1950 to 2020. *Acta Scientiae Circumstantiae*, *43*(6), 203–214. https://doi.org/10.13671/j.hjkxxb.2022.0403

Liang, Y. (2012b). *Investigation and evaluation of red tide disaster in China (1933–2009)*. China Ocean Press.

Liu, F. (2008). Analysis of the current situation of the marine environment in Taozi Bay. *Ocean Development and Management*, *25*(6), 96–98.

Liu, J., Xia, J., Zhuang, M., Zhang, J., Sun, Y., Tong, Y., Zhao, S., & He, P. (2021). Golden seaweed tides accumulated in *Pyropia* aquaculture areas are becoming a normal phenomenon in the Yellow Sea of China. *Science of the Total Environment*, *774*, 145726. https://doi.org/10.1016/j.scitotenv.2021.145726

Ma, Y., Xing, H., Song, X., Zhang, X., Sun, S., Dai, Z., Tao, H., & Gu, W. (2010). The basic situation and response measures of green tide outbreak in Yantai Golden Beach. *Shandong Fisheries*, *27*(4), 10–12.

Met Office Marine Data Bank. http://www.metoffice.gov.uk/hadobs/hadisst/data/download.html

NOAA. https://oceancolor.gsfc.nasa.gov/l3/

Qi, L., Hu, C., Wang, M., Shang, S., & Wilson, C. (2017b). Floating algae blooms in the East China Sea. *Geophysical Research Letters*, *44*(22), 11501–11509. https://doi.org/10.1002/2017GL075525

Song, M., Yan, T., Kong, F., Wang, Y., & Zhou, M. (2022). Increased diversity and environmental threat of harmful algal blooms in the Southern Yellow Sea, China. *Journal of Oceanology and Limnology*, *40*(6), 2107–2119. https://doi.org/10.1007/s00343-021-1209-4

Song, X., Fu, P., Jiang, X., Liu, L., Liu, A., Cheng, L., Dong, Z., & Ma, Y. (2021). Characteristics and trends of typical ecological disasters in coastal waters of Shandong Province. *Ocean Development and Management*, *28*(6), 31–36.

Wei, W., Du, H., Jiang, P., Lin, X., Cai, D., & Ding, L. (2011b). *Overview of the first green tide outbreak in the Nan'ao sea area of eastern Guangdong in 2011*. Collection of Abstracts of the Eighth Member Congress and Sixteenth Academic Symposium of the Chinese Psychological Society.

Xiao, J., Wang, Z., Liu, D., Fu, M., Yuan, C., & Yan, T. (2021b). Harmful macroalgal blooms (HMBs) in China's coastal water: Green and golden tides. *Harmful Algae*, *107*, 102061. https://doi.org/10.1016/j.hal.2021.102061

Xing, Q., Guo, R., Wu, L., An, D., Cong, M., Qin, S., & Li, X. (2017b). High-resolution satellite observations of a new hazard of golden tides caused by floating *Sargassum* in winter in the Yellow Sea. *IEEE Geoscience and Remote Sensing Letters*, *14*(10), 1815–1819. https://doi.org/10.1109/LGRS.2017.2737079

Xing, Q., & Hu, C. (2016b). Mapping macroalgal blooms in the Yellow Sea and East China Sea using HJ-1 and Landsat data: Application of a virtual baseline reflectance height technique. *Remote Sensing of Environment*, *178*, 113–126. https://doi.org/10.1016/j.rse.2016.02.065

Xiong, Y., Gao, L., Qu, L., Xu, J., Ma, Z., & Gao, G. (2022b). The contribution of fish and seaweed mariculture to the coastal fluxes of biogenic elements in two important aquaculture areas, China. *Science of the Total Environment*, *856*, 159056. https://doi.org/10.1016/j.scitotenv.2022.159056

Zeng, B., Sun, Y., Song, W., Wang, Z., & Zhang, X. (2023b). Recurrence of the green tide in the Bohai Sea, China: A green tide caused by coastal reclamation projects. *Journal of Sea Research*, *191*, 102333. https://doi.org/10.1016/j.seares.2022.102333

Zhang, L., Yang, Y., He, W., Xu, J., & Li, R. (2022b). Fluxes of riverine nutrient to the Zhujiang River estuary and its potential eutrophication effect. *Acta Oceanologica Sinica*, *41*(6), 88–98. https://doi.org/10.1007/s13131-021-1919-7

Zhao, D. (2010b). *Occurrence regularity of red tide disaster in typical sea areas of China*. China Ocean Press.

Zheng, L., Wu, M., Zhao, J., Wang, D., Zhou, M., & Zhao, L. (2022b). Remote sensing monitoring and temporal and spatial distribution characteristics of gold tide in the South Yellow Sea. *Haiyang Xuebao*, *44*(5), 12–24. https://doi.org/10.12284/hyxb2022095

SUPPORTING INFORMATION

Additional supporting information can be found online in the Supporting Information section at the end of this article.

How to cite this article: Feng, Y., Xiong, Y., Hall-Spencer, J. M., Liu, K., Beardall, J., Gao, K., Ge, J., Xu, J., & Gao, G. (2023). Shift in algal blooms from micro- to macroalgae around China with increasing eutrophication and climate change. *Global Change Biology*, *00*, e17018. https://doi.org/10.1111/gcb.17018